

1 *Supplementary information for*

2 **Hydroxyl-assisted iodine ions intercalating  $\text{Bi}_2\text{O}_2\text{CO}_3$  nanosheets to**  
3 **construct the interlayered bridge for enhanced photocatalytic**  
4 **activity of phenol**

5 **1. Tables**

6 **Table S1.** Reaction conditions and final phase of products.

7 **Table S2.** Structure parameters of  $\text{Bi}_2\text{O}_2\text{CO}_3$ .

8 **2. Figures and results**

9 **Figure S1.** XRD and SEM images of products obtained in different solvents.

10 **Figure S2.** Solvent effects on the phase of products.

11 **Figure S3.** DFT calculation of the band structure of  $\text{Bi}_2\text{O}_2\text{CO}_3$  and  $\text{Bi}_2\text{O}_2\text{CO}_3$ .

12 **1. Tables**13 **Table S1.** Reaction conditions and final phase of products.

No.	Solvent	Solvent ratio	Bi(NO <sub>3</sub> ) <sub>3</sub> •5H <sub>2</sub> O (mmol)	Urea (g)	KI (mmol)	Phase of products
1	H <sub>2</sub> O	-	2	1	4	I-Bi <sub>2</sub> O <sub>2</sub> CO <sub>3</sub>
2	EG	-	2	1	4	Bi <sub>4</sub> O <sub>5</sub> I <sub>2</sub>
3	Et and EG	8:2	2	1	4	BiOI
4	EG and H <sub>2</sub> O	1:9	2	1	4	I-Bi <sub>2</sub> O <sub>2</sub> CO <sub>3</sub>
5	EG and H <sub>2</sub> O	2:8	2	1	4	I-Bi <sub>2</sub> O <sub>2</sub> CO <sub>3</sub>
6	EG and H <sub>2</sub> O	5:5	2	1	4	I-Bi <sub>2</sub> O <sub>2</sub> CO <sub>3</sub>
7	EG and H <sub>2</sub> O	2:8	2	1	-	Bi <sub>2</sub> O <sub>2</sub> CO <sub>3</sub>
8	Et and H <sub>2</sub> O	2:8	2	1	4	Bi <sub>2</sub> O <sub>2</sub> CO <sub>3</sub> & BiOI
9	Et and H <sub>2</sub> O	5:5	2	1	4	Bi <sub>2</sub> O <sub>2</sub> CO <sub>3</sub> & BiOI
10	Et and H <sub>2</sub> O	8:2	2	1	4	Bi <sub>2</sub> O <sub>2</sub> CO <sub>3</sub> & BiOI
11	Et and H <sub>2</sub> O	9:1	2	1	4	BiOI

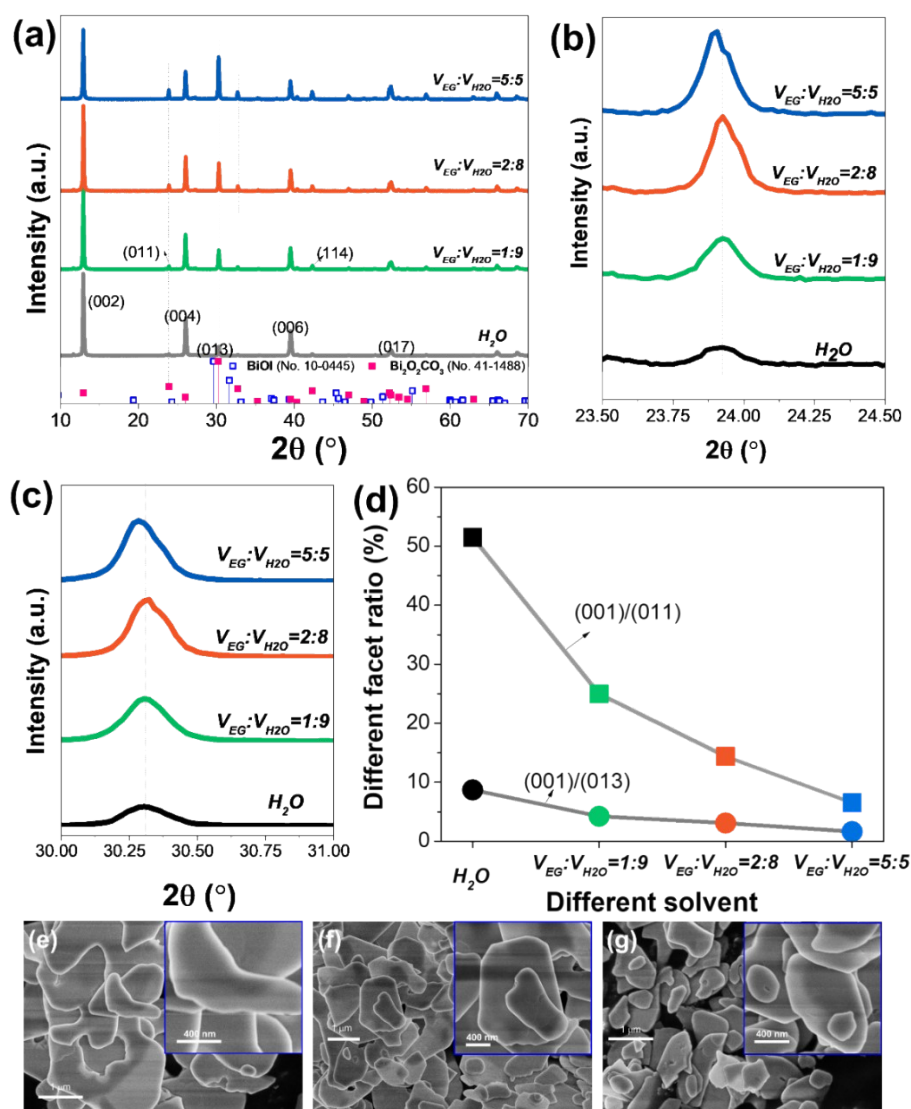
14

No.		a (Å)	b (Å)	c (Å)	α (°)	β (°)	γ (°)	V (Å <sup>3</sup> )	Bandgap (eV)
1	Bi <sub>2</sub> O <sub>2</sub> CO <sub>3</sub>	5.56958	28.07291	5.54626	90	90	90	867.1814	1.98
2	Bi <sub>2</sub> O <sub>2</sub> CO <sub>3</sub> I <sub>4</sub>	5.89126	33.05380	6.37392	90	90	90	1241.1840	0

15 **Table S2.** Structure parameters of Bi<sub>2</sub>O<sub>2</sub>CO<sub>3</sub>.

16

## 17 2. Figures and results

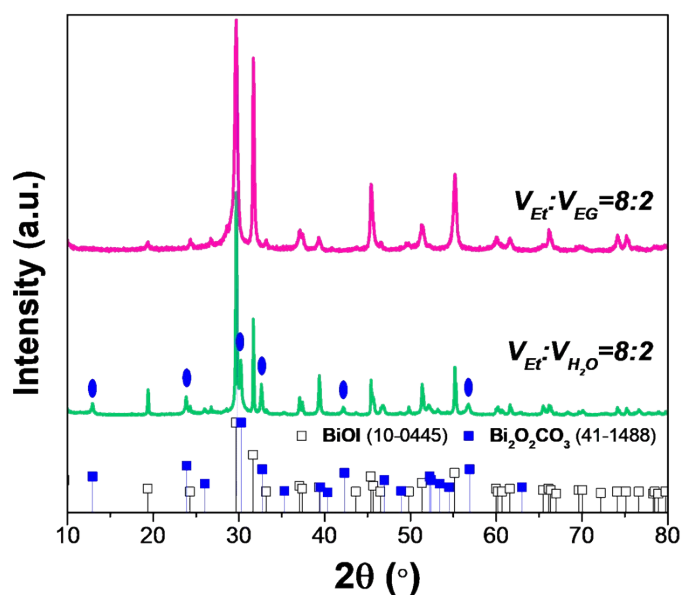


18

19 **Fig. S1.** (a) XRD patterns of samples obtained from different solvents, local magnified  
 20 XRD patterns of (b) (011) and (c) (013) planes. (d) Different plane ratio of (001)/(011)  
 21 and (001)/(013).

22 According to **Fig. S1**, the water was of benefit to the formation of  $Bi_2O_2CO_3$ , while  
 23 the hydroxyl groups of solvent was contributed to the generation of BiOI. Employing  
 24 EG and water mixture as solvent and altering the volume of EG in the mixture, the  
 25 resulted XRD patterns of products were showed in **Fig. 1a**. In the pure  $H_2O$ , all the  
 26 characteristic peaks were indexed to the tetragonal  $Bi_2O_2CO_3$  (JCPDS No. 41-1455)

27 although the concentration of KI was relatively high. By reducing the volume of H<sub>2</sub>O  
28 and increasing the volume of EG correspondingly, the XRD patterns without impurity  
29 characteristic peaks were also obtained, which were indexed to Bi<sub>2</sub>O<sub>2</sub>CO<sub>3</sub>. But, partial  
30 characteristic peaks of resulted Bi<sub>2</sub>O<sub>2</sub>CO<sub>3</sub> were shifted to lower 2θ when altering the  
31 volume ratio of EG and water, as magnified some local characteristic peaks. Especially,  
32 when the volume of EG increasing over 50% of the mixed solvent, such as, the 2θ  
33 corresponded to (011) and (013) planes of Bi<sub>2</sub>O<sub>2</sub>CO<sub>3</sub> were down-shifted significantly  
34 (**Fig. 1b** and **1c**). The down-shifted characteristic peaks indicated that the crystal  
35 structure of Bi<sub>2</sub>O<sub>2</sub>CO<sub>3</sub> was expanded due to the intercalation of iodine ions into the  
36 structure of Bi<sub>2</sub>O<sub>2</sub>CO<sub>3</sub> <sup>1, 2</sup>. Furthermore, the intensity of some characteristic peaks  
37 increased gradually when increasing the volume ratio of EG. For instance, the planes  
38 ratio value of (001)/(011) and (001)/(013), were decreased by increasing the volume of  
39 EG. Especially, the value of (001)/(011) decreased dramatically, implying that the (011)  
40 planes in the final products increased when increasing the volume ratio of EG in the  
41 mixed solvent (**Fig. 1d**). All the products were maintained in 2D sheet-like morphology,  
42 regardless of the volume ratio of H<sub>2</sub>O and EG. But, the size and morphology of the  
43 products were slightly adjusted. In the pure water, the resulted sheets present much  
44 irregular shape and the size of final Bi<sub>2</sub>O<sub>2</sub>CO<sub>3</sub> sheets was over microscale (**Fig. 2a**).  
45 When decreasing the volume of water and increasing the volume of EG simultaneously,  
46 the size of products was decreased from ~3 μm to ~800 nm (**Fig. 2b** to **2d**). Because,  
47 increasing the volume of EG will increase the viscosity of solvent, depressing the  
48 corresponding growth rate of products and forming smaller size of products <sup>3</sup>.  
49 Apparently, massive hydroxyl groups stemmed from EG played distinctive role on the  
50 structure expansion of Bi<sub>2</sub>O<sub>2</sub>CO<sub>3</sub> and size regulation.



51

52

**Fig. S2.** XRD patterns of different products.

53 Fixing the volume ratio of Et but altering another solvent, the final phase of products was

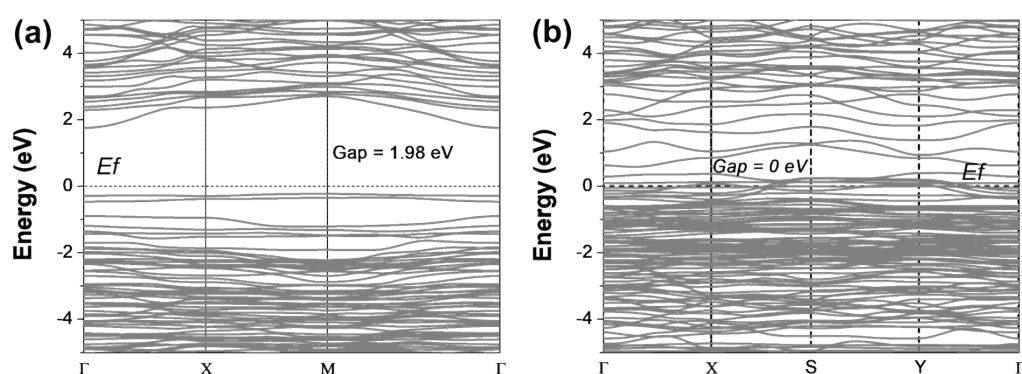
54 significantly different (**Figure S2**). When selecting water to mix with Et, the final products

55 were mixed phase of BiOI (JCPDS No. 10-0445) and  $\text{Bi}_2\text{O}_2\text{CO}_3$  (JCPDS No. 41-1488)

56 caused by the different reaction rate of BiOI and  $\text{Bi}_2\text{O}_2\text{CO}_3$  (**Fig. 1b**). Comparatively,

57 employing EG to replace water, the final phase of products was homogenous one that only

58 tetragonal BiOI (JCPDS No. 10-0445) were obtained.



59

60

**Fig. S3.** Calculated band structure of (a)  $\text{Bi}_2\text{O}_2\text{CO}_3$  and (b) I- $\text{Bi}_2\text{O}_2\text{CO}_3$ .

## 61 References

62 1 Y. X. Xing, J. Zhang, Z. L. Liu, C. F. Du, Steering photoinduced charge kinetics via  
 63 anionic group doping in  $\text{Bi}_2\text{MoO}_6$  for efficient photocatalytic removal of water organic  
 64 pollutants, *Rsc Advances*, 2017, **7**, 35883-35896.

65 2 L. Liang, J. Cao, H. L. Lin, X. M. Guo, M. Y. Zhang, S. F. Chen, Enhancing visible  
66 light photocatalytic and photocharge separation of  $(\text{BiO})_2\text{CO}_3$  plate via dramatic I<sup>-</sup> ions  
67 doping effect, *Materials Research Bulletin*, 2016, **80**, 329-336.  
68 3 W. W. Zhou, B. Yan, C. W. Cheng, C. X. Cong, H. L. Hu, H. J. Fan, T. Yu, Facile  
69 synthesis and shape evolution of highly symmetric 26-facet polyhedral microcrystals of  $\text{Cu}_2\text{O}$ ,  
70 *Crystengcomm*, 2009, **11**, 2291-2296.

71